Opto-Electronic Advances

Supplementary information

2019, Vol. 2, No. 3

DOI: 10.29026/oea.2019.180023

All-metallic wide-angle metasurfaces for multifunctional polarization manipulation

Xiaoliang Ma[1,2], Mingbo Pu[1,2], Xiong Li[1,2], Yinghui Guo[1] and Xiangang Luo[1,2]*

[1]State Key Laboratory of Optical Technologies on Nano-Fabrication and Micro-Engineering, Institute of Optics and Electronics, Chinese Academy of Sciences, Chengdu, 610209, China; [2]School of Optoelectronics, University of Chinese Academy of Sciences, Beijing 100049, China
* Correspondence: X G Luo, E-mail: lxg@ioe.ac.cn

This file includes:

Supplementary information for this paper is available at https://doi.org/10.29026/oea.2019.180023

Section 1: Pseudo-Brewster angle

For the reflection occurring at a smooth surface between two different materials with refractive indexes of n_1 and n_2, the reflectance of p polarized light can be alternatively written as:

$$R_p = \frac{\tan^2\left(\theta_i - \theta_t\right)}{\tan^2\left(\theta_i + \theta_t\right)} \quad , \tag{S1}$$

where θ_i and θ_t are the incidence and transmission angles. The condition for zero refletion for p-polaizred light is:

$$\theta_i + \theta_t = 90° \quad , \tag{S2}$$

here $\theta_i = \theta_B$ is called the Brewster angle. Using the Snell's law,

$$n_1 \sin\theta_B = n_2 \sin\theta_t \quad . \tag{S3}$$

One can obtain

$$\theta_B = \arctan\left(n_2 / n_1\right) = \arctan\left(n_{21}\right) \quad . \tag{S4}$$

When n_{21} is a complex, the Brewster angle θ_B would also have an imaginary part. In this case, the real part of θ_B is termed the pseudo-Brewster angle. If the substrate is thick enough, all transmitted p-polarized light would be finally absorbed by the substrate, resulting a distinct thermal radiation, as demonstrated in this paper.

Section 2: Impedance model of the corrugated metal surface

The Fresnel's equations can be also interpreted by the impedance theory and transfer matrix method. In general, the impedances for air and metal can be written as:

$$Z_{\text{Air}} = \frac{E_{\parallel}}{H_{\parallel}} = \begin{cases} \dfrac{E_0}{H_0 \cos\theta} = \dfrac{Z_0}{\cos\theta}, & s \\ \dfrac{\sqrt{E_0^2 - E_z^2}}{H_0} = Z_0 \cos\theta, & p \end{cases} , \tag{S5}$$

and

$$Z_{\text{Metal}} = \begin{cases} \dfrac{Z_0}{\sqrt{\varepsilon_m - \sin^2\theta}}, & s \\ \dfrac{Z_0\sqrt{\varepsilon_m - \sin^2\theta}}{\varepsilon_m}, & p \end{cases} , \tag{S6}$$

where $E_{\parallel}$ and $H_{\parallel}$ are the horizontal components of the electric/magnetic fields, E_0 and H_0 are the electric/magnetic field amplitudes of the incident plane wave. Obviously, the impedance matching for p-polarization is a direct result of the increase of E_z along with the rise of incidence angle. As a result, it is critical to reduce E_z in order to eliminate the pseudo-Brewster effect.

We note that the posts array act as normal dielectric for s-polarized wave, while behave like a waveguide array for p-polarized wave. In this case, the effective impedances and wave numbers can be written as

$$Z_{\text{eff}}^{s} = Z_0 / \cos\theta \quad , \tag{S7}$$

$$k_{z,\text{eff}}^{s} = k_0 \cos\theta \quad , \tag{S8}$$

for s-polarization, and

$$Z_{\text{eff}}^{p} = Z_0 \quad , \tag{S9}$$

$$k_{z,\text{eff}}^{p} = k_0 \quad , \tag{S10}$$

for p-polarization.

The optical performance of the air-posts-metal configuration can be calculated using transfer matrix method:

$$\begin{bmatrix} a \\ b \end{bmatrix} = \frac{1}{2}\begin{bmatrix} 1 + Z_{\text{air}}/Z_{\text{eff}} & 1 - Z_{\text{air}}/Z_{\text{eff}} \\ 1 - Z_{\text{air}}/Z_{\text{eff}} & 1 + Z_{\text{air}}/Z_{\text{eff}} \end{bmatrix} \begin{bmatrix} \exp(-\mathrm{i}k_{z,\text{eff}}h) & 0 \\ 0 & \exp(\mathrm{i}k_{z,\text{eff}}h) \end{bmatrix} \begin{bmatrix} 1 \\ (Z_m - Z_{\text{Air}})/(Z_{\text{Metal}} + Z_{\text{Air}}) \end{bmatrix}, \tag{S11}$$

where h is the thickness of the posts, $(Z_m - Z_{\text{Air}})/(Z_{\text{Metal}} + Z_{\text{Air}})$ is the reflection of thick metal layer. The reflection coefficient can be then directly calculated using b/a.

Since the difference between the impedances of air and the posts array (p-polarization) increases with the incidence angle, the reflectance would increase correspondingly. As a result, the pseudo-Brewster effect can be eliminated.

Section 3: Influence of the geometric parameters on the crypsis performance

The dependence of the reflectance on the geometric parameters is investigated using FEM simulations. Figs. S7–S9 depict the reflectance spectra for different configurations (widths, heights and periods). It is obvious that these geometric parameters have relatively small influence on the performance when they are varied from the optimized values. The parameters used for fabrication are chose by minimizing the fabrication difficulty.

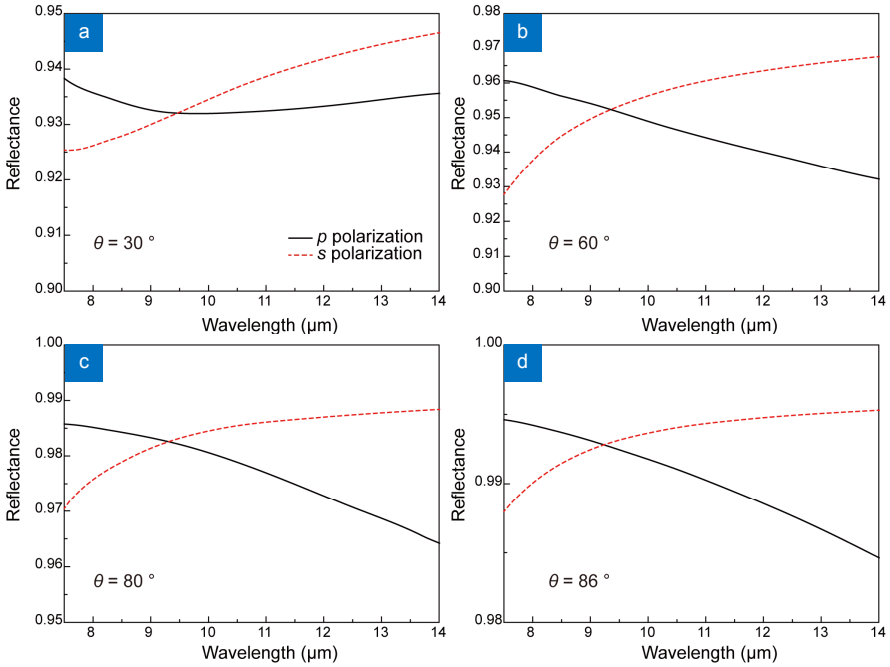

Fig. S1 | Simulated reflectance of the Au Sample (*p* = 3 μm, *w*=1.25 μm, *h*=1.9 μm). (**a**) *θ*=30°. (**b**) *θ*=60°. (**c**) *θ*=80°. (**d**) *θ*=86°.

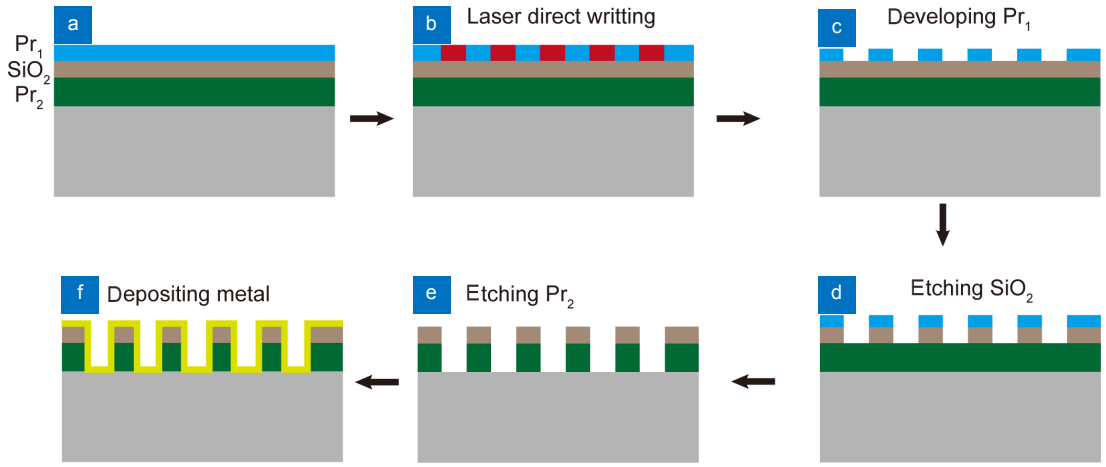

Fig. S2 | Schematic of the fabrication process. (**a**) Preparation of the three-layer films comprised of a thick photoresist (Pr_2), an intermediate SiO_2 layer and a thin photoresist layer (Pr_1). (**b**) Laser direct writing of the top resist layer. (**c**) Development of the top resist layer. (**d**) Etching of the SiO_2 intermediate layer. (**e**) Etching of the bottom resist layer. (**f**) Depositing of 200 nm thick metal.

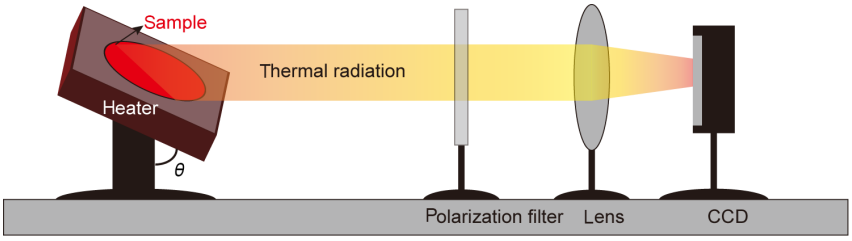

Fig. S3 | Set-up of the thermal polarimetric imaging system.

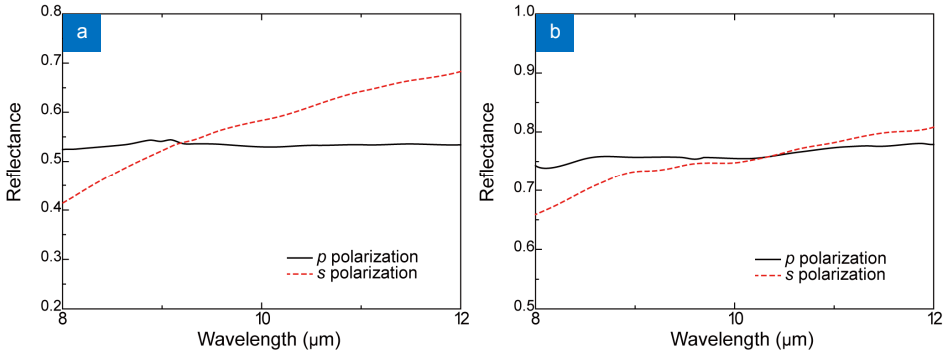

Fig. S4 | Measured polarimetric reflectance of the Cr Sample. (**a**) θ = 70°. (**b**) θ = 80°. The increased absorption compared to the Au sample is attributed to the larger ohmic loss as well as the deformation of the Cr coating, as can be seen in Fig. 3(d).

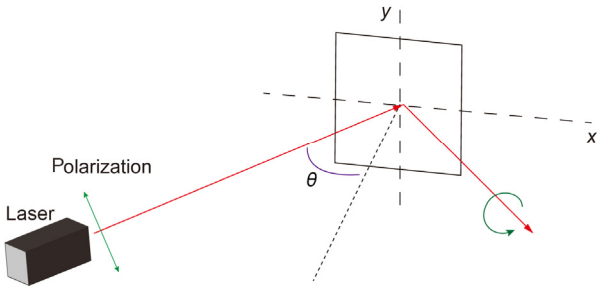

Fig. S5 | Schematic of the measurement process of the elliplicity.

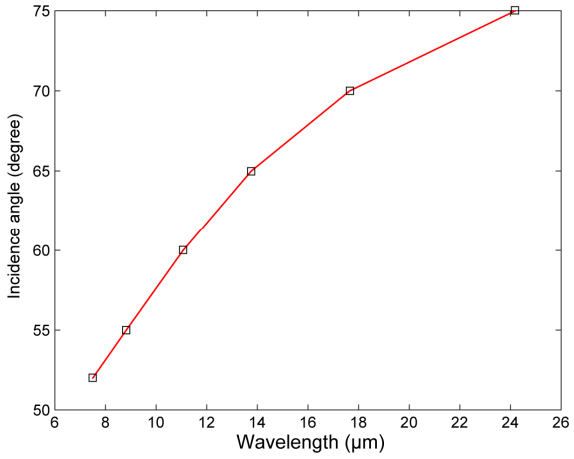

Fig. S6 | Broadband operation of the reflective waveplate. The operating wavelength can be tuned by varying the incidence angle.

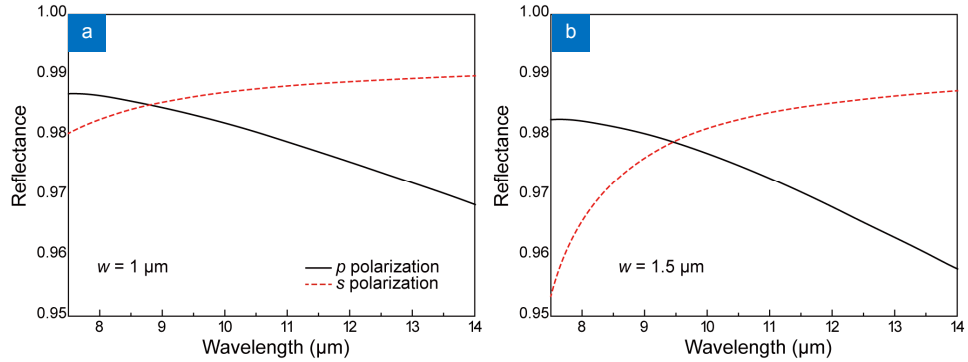

Fig. S7 | Influence of the posts width on the reflectance (*θ*=80°). (a) *p*=3 μm, *w*=1 μm, *h*=1.9 μm. (b) *p*=3 μm, *w*=1.5 μm, *h*=1.9 μm.

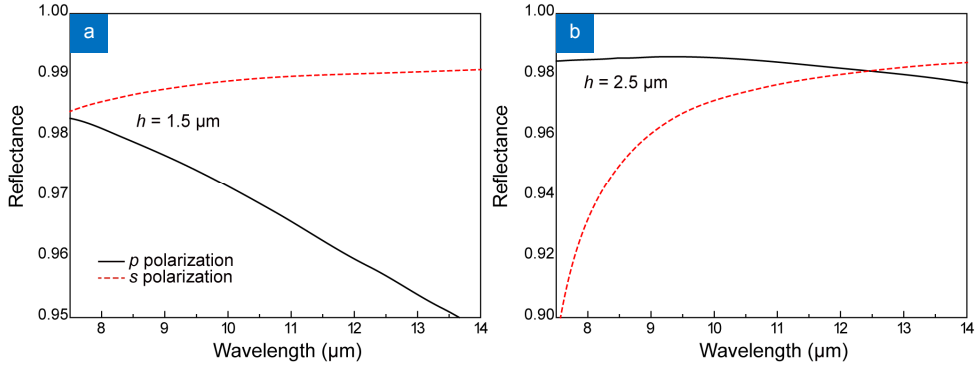

Fig. S8 | Influence of the posts height on the reflectance (*θ*=80°). (a) *p*=3 μm, *l*=1.25 μm, *h*=1.5 μm. (b) *p*=3 μm, *l*=1.25 μm, *h*=2.5 μm.

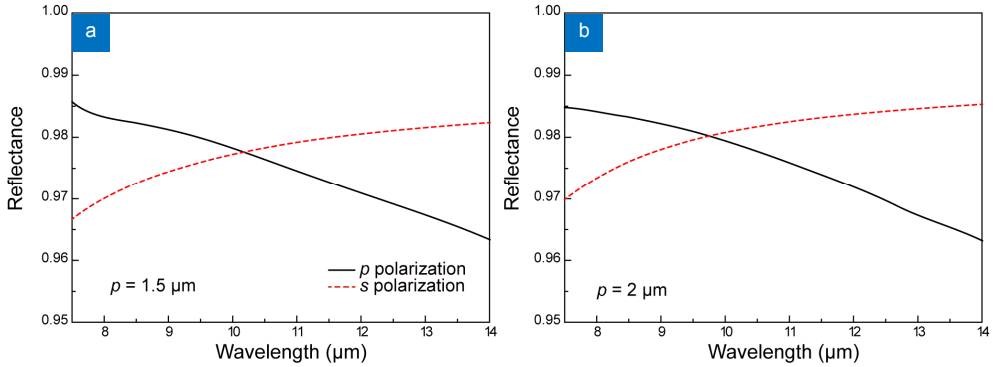

Fig. S9 | Influence of the posts period on the reflectance (*θ*=80°). (**a**) *p*=1.5 μm, *l*=0.5 μm, *h*=1.9 μm. (**b**) *p*=2 μm, *l*=0.75 μm, *h* = 1.9 μm.